Kinetic study of crystallisation of sol-gel derived calcia-alumina binary compounds

Marjan Zahedi, Nima Roohpour and Asim K. Ray[1]
School of Engineering and Materials Science, Queen Mary, University of London,
Mile End Road London E1 4NS

Abstract

In-situ High Temperature X-Ray Diffraction (HTXRD) and Differential Scanning Calorimetric (DSC) studies were performed on a sol-gel derived binary compound of a calcia-alumina (C12A7) system consisting of calcium oxide (CaO) and aluminum oxide (Al_2O_3) in a ratio of 12:7 for in-situ investigation into the phase transformations under progressively increasing thermal activation from room-temperature to 1200°C. The crystallisation of amorphous samples formulated at room-temperature on magnesium oxide (MgO) single crystal (100) substrates was found to be complete on heat treatment at 1100°C for 3 hours. This observation was further supported by independent Fourier Transform Infrared (FTIR) and Raman Spectroscopies. Values of 348 kJ/mol and 375 kJ/mol were estimated from Kissinger plots for activation energies of crystallisation of CaO and Al_2O_3 constituents, respectively.

Keywords: sol-gel growth, heat treatment, Fourier transform infrared spectroscopy (FTIR), Raman spectroscopy and scattering, thermogravimetric analysis (TGA), crystallisation,

[1] Present address: The Wolfson Centre For Materials Processing, Brunel University, Uxbridge, Middlesex UB8 3PH, UK Direct Line +44 (0)1895 267794, Fax +44 (0)1895 269737, Email asim.ray@brunel.ac.uk

1. Introduction

Transparent oxides are extensively used in a wide range of applications in electronic and optoelectronic systems including fully transparent high performance transistors, ultraviolet (UV) light emitting diodes (LED) [1], invisible circuits [2], flat-panel displays, solar cells [3] and energy conservation (smart windows) devices [4]. One promising transparent oxide that can be used as an insulating, semiconducting or metallic layer, is the zeolite-like metal oxide compound $12CaO.7Al_2O_3$ (C12A7). This novel oxide exhibits physically interesting properties by exploiting its high-density intrinsic defect nanostructure [5].

The crystal growth of C12A7 is similar to that of zeolite crystals, where the oxygen ions work as templates to grow the framework. Unlike zeolite crystals, these oxygen ions remain inside the crystal as free ions trapped inside nano-sized cages. In each unit cell the framework is composed of 116 atoms in the form of 12 Ca-O-Al cages, capable of taking up two O^{2-} ions into its structure. The cages have an entrance of 0.1nm in diameter, which controls the elemental substitution within the cages. Only a limited number of ions meet the criteria to be substituted for the oxygen ions, inducing a wide range of exceptional characteristics into this oxide material [6-8]. C12A7 single nanoparticles have been synthesized through different routes including solid-state reaction at high temperature [9] and self-propagating combustion at low temperature [10]. We have recently reported the synthesis of C12A7 thin films on magnesium oxide (MgO) single crystal (100) substrates using room temperature sol-gel technique [11]. The partial crystallisation of the C12A7 thin film was observed at 800 ^{0}C and the crystallisation was completed on heat treatment at 1100 ^{0}C for 3 hours. UV-visible optical spectra showed two absorption peaks at 5.3eV and 6.1eV. The peak at 5.3eV is believed to be associated with an O^{2-} - Cage Conduction Band type transition whereas the Framework Valence Band to Framework Conduction Band transition was found to be responsible for the peak at 6.1eV [12]. This sol-gel route produces crystalline C12A7 nanoparticles loaded with O^{2-} /OH^- ions through hydrolysis and condensation process of precursor materials. The mono-dispersed, stable solution formed undergoes a series of chemical reactions and phase transformations during hydrolysis, condensation and thermal treatment. In this present investigation, an attempt has been made to study the effect of the heating rate on crystallisation behavior and the activation energy of structural relaxation and crystallisation has been determined. The peak temperature of crystallisation is known to depend strongly upon the heating rate [13].

This paper reports the results of in situ X-Ray diffraction studies on the C12A7 samples as they were vacuum annealed at different rates by progressively increasing the temperature from 25 ^{0}C to 1200 ^{0}C. Differential scanning calorimetric (DSC) studies were performed to investigate the crystallisation behavior. Further evidence for crystallisation of sol-gel synthesised C12A7 materials was obtained from FTIR and Raman spectroscopies. A range of chemical reactions and phase transformations was identified through these structural and analytical characterisations to be associated with sol-gel synthesis of C12A7, building on our previous work in this field of study [11].

2. Experimental

The method consists of the preparation of binary compound of a calcia-alumina (C12A7) from appropriate chemicals and spectroscopic studies for phase changes.

2.1 Materials

Aluminum sec-butoxide ($Al[OCH(CH_3)C_2H_5]_3$) known as ($Al(OBu)_3$) with purity of 99.99% , ethyl acetoacetate ($CH_3COCH_2COOC_2H_5$) known as Etac with purity of ≥90.0% , calcium nitrate tetrahydrate ($Ca(NO_3)_2 \cdot 4H2O$) with purity of ≥90.0%, hydrochloric acid 1M (HCl) and ethanol (CH_3CH_2OH) with purity of ≥98.0%, all chemicals were purchased from Sigma Aldrich Chemicals Ltd., UK.

2.2 Sol-Gel synthesis of C12A7

C12A7 sol was synthesized through hydrolysis of two separate solutions. Aluminium oxide hydroxide (AlOOH) sol was prepared using aluminium sec-butoxide $Al(OBu)_3$ as the precursor. In order to avoid precipitation this precursor was modified using ethyl acetoacetate (Etac), forming $Al(OBu)_3$ that is hydrolytically unstable and its hydrolysis leads to immediate precipitation. However, the modification of $Al(OBu)_3$ using ethyl acetoacetate (Etac) mediates the hydrolysis of Al^{3+} ions, through substitution of monodentate butoxy ligands of $Al(OBu)_3$ with Etac groups. Etac groups will be bonded to Al atoms in an enolic form [14].

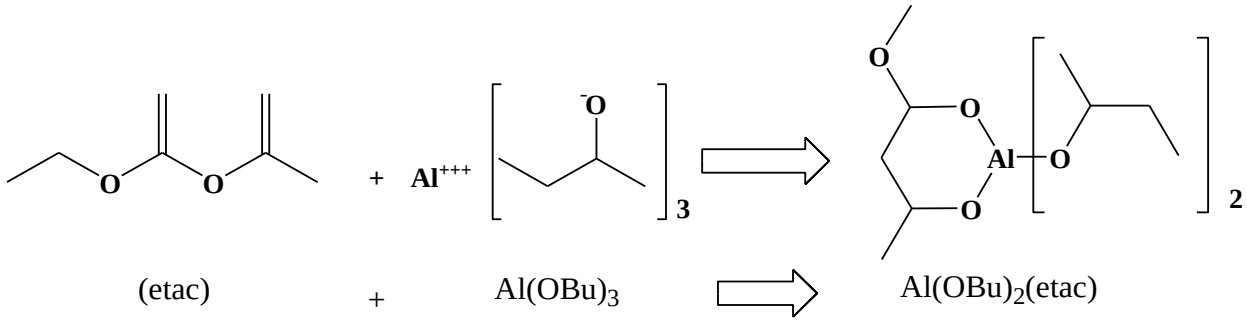

$Al(OBu)_3$ was mixed with Etac with a molar ratio of $Al(OBu)_2$: Etac = 1:1. The mixture was magnetically stirred for 30 minutes followed by 1 hour of ultrasonic mixing in an Ultrawave U50 Bath for 1 h in order to achieve the formation of a stable transparent C12A7 solution. An $Al(OBu)_2$ (Etac) complex was formed through this stage. This new precursor was diluted with ethanol ($Al(OBu)_2$: ethanol = 1:4) prior to hydrolysis. In the final step, distilled water was diluted with ethanol followed by pH regulation using hydrogen chloride (HCl) acid and ($Al(OBu)_3$: H_2O :HCl = 1: 3: 0.15). Diluted distilled water was then added to the $Al(OBu)_2$ (Etac) solution initiating the hydrolysis process. The hydrolysis was performed under vigorous stirring using an ultrasonic bath at 1000Hz, followed by gentle stirring (~400 r.p.m) at room temperature for 24 hours using a RCT basic safety control IKAMA magnetic stirrer. During hydrolysis of the modified $Al(OBu)_2$(Etac) compound, Etac groups will be separated from the compound in both enolic and ketonic forms. Following the separation of butoxy ligands, AlO bonding will be exposed to OH bonding of water, resulting in the formation of boehmite ((γ-AlO(OH))). The reaction at this water content may be derived as:

$$Al(OC_4H_9)_2(etac) + 3H_2O \rightarrow AlOOH(H_2O) + etac + 2C_4H_9OH$$

The acid concentration used in the synthesis of AlOOH particles was chosen at molar ratio of $Al(OBu)_3$: HCl = 1 : 0.15, thereby reducing the pH of the solution from 10.4 to 8 [15,16], well below the isoelectric point of boehmite particles. Such acid regulation will reduce the chance of agglomeration due to Columbic interactions between particles [17, 18]. The final product was AlOOH molecules dissolved in ethanol. A second solution was prepared using $Ca(NO_3)_2$. $4H_2O$ dissolved in ethanol. Additional water was added to the solution ($Ca(NO_3)_2$, $4H_2O$: H_2O = 3:4) to initiate partial hydrolysis. Addition of water expels some salt ions to form HNO_3, decreasing the pH of the solution to 4 [6]. The dispersion of calcium nitrate in the solvent was facilitated using an ultrasonic bath (1000 Hz) followed by 24 hours of magnetic stirring (400 r.p.m). The solution formed required no further acid addition since HNO_3 was formed within the solution.

The sol-gel process starts with a homogenous solution of AlOOH and $Ca(NO_3)_2$ in ethanol solvent with the concentrations meeting the nominal composition of C12A7 compound. The AlOOH and $Ca(NO_3)_2$ solution were mixed allowing the formation of a homogenous C12A7 amorphous solution. C12A7 nanoparticles were prepared by dispensing a thin layer of sol in a petri dish followed by a 72 hour drying process at room temperature. During drying, evaporation of ethanol progressively facilitates the formation of an amorphous phase from the solution. Continued drying

of the sol and evaporation of the solvent promotes the inorganic precursors and organic additives into the desired structure. The powders were then subjected to a heat treatment at ambient atmosphere with the annealing temperature set to 1100°C for the duration of 3 hours. Thermal treatment of the dried gel at 1100°C will lock in the nano-caged structure of C12A7 and develops covalent bonds of Ca-O-Al to form the framework. The crystalline C12A7 formed along with amorphous C12A7 dried gels were used for various characterizations.

2.3 Characterisation

High Temperature X-Ray Diffraction (HTXRD) was performed at variable temperature using a D5000 X-Ray diffractometer equipped with an Anton Paar HTK-16 vacuum furnace using CuKα radiation (λ=1.54A°). An Anton Parr TCU 2000 temperature control unit provided direct temperature control. The detector was a Panalytical X'Celerator solid-state detector, which scans continuously. Samples were placed on a pre-stressed platinum strip. Experiments were performed from room temperature up to 1200°C with a heating rate of 10°C/min, in the 5°-65° 2θ domain. The dried C12A7 gel was placed in a small crucible and fitted inside the STA1500 (Thorn Scientific, UK) differential scanning calorimeter (DSC) and exposed to heat treatment at various rates over a programmed temperature range from 25°C to 1200°C.

Fourier transform infrared spectroscopy (FTIR) measurements were carried out using a Nicolet 8700 FTIR spectrometer (Thermo Electron Corporation, UK) in conjunction with an MTEC Photoacoustic Spectrum (PAS) cell. Spectra were obtained in the mid infrared region (4000-400 cm^{-1}) at 4 cm^{-1} resolution and averaging of 256 scans on two different samples; one with amorphous C12A7 dried gel and the other with crystallized C12A7 powder.

Raman Spectroscopy was carried out using a Nicolet Almega XR dispersive Raman spectrophotometer (Thermo Fisher Scientific, Madison Wisconsin, USA), equipped with 532nm and 785nm lasers on two different samples; one with amorphous C12A7 dried gel and the other with crystallized C12A7 powder. All the spectra were collected in the range of 400 cm^{-1}-4000cm^{-1} using a 10X objective and over an average of 256 scans, with 1 second exposure time at low resolution.

3. Results and discussions

3.1 HTXRD and DSC

Figure 1 shows a sequence of data collected from the HTXRD performed on amorphous C12A7 dried gel in the temperature range of 25°C-1200°C. The phase transformations at different

stages of thermal treatment are depicted in Figure 2 as DSC patterns at three different heating rates of 5°C/min, 10°C/min and 20°C/min from room temperature to 1200°C. During the sol-gel process, two distinct compounds, calcium nitrate ($Ca(NO_3)_2$) and aluminium oxide hydroxide (AlOOH) have been formed at room temperature. $Ca(NO_3)_2$ is a metallic salt and exists as a cubic crystalline phase in primitive cubic space group P213 at room temperature. This structure is depicted in Figure 1 with the diffraction pattern at 100°C fitting the one for $Ca(NO_3)_2$ collected from International Centre for Diffraction Database. This pattern remains strictly identical to the one for $Ca(NO_3)_2$ up to 500 °C. As observed in the DSC pattern, the tetrahydrate molecule attached to $Ca(NO_3)_2$ boiled off giving rise to an endothermic peak at 180°C -230°C depending on the heating rate [19]. Calcium nitrate will undergo a continuous decomposition process from 250°C – 550°C, during which $Ca(NO_3)_2$ is decomposed to CaO [20,21]. This event is completed at 500°C -560°C with a strong endothermic peak at various heating rates. The phase transformation is also confirmed with the disappearance of the diffraction pattern of $Ca(NO_3)_2$ at 600°C. This phase is then crystallized at 820°C -850°C with the appearance of an exothermic peak in the DSC trace. AlOOH present in the sol will not undergo any crystallisation during our thermal treatment, with no evidence of such crystallisation observed in both XRD and DSC patterns. AlOOH is directly transferred to γ-Al_2O_3 with the appearance of an endothermic peak at 380°C -430°C [22]. These results indicate the endothermic nature of this phase transformation. At 950°C -990°C the appearance of an exothermic peak illustrates the crystallisation of γ-Al_2O_3 and its transformation to α-Al_2O_3 [23,24]. C12A7 crystal phase is formed when CaO and α-Al_2O_3 crystals grow and interact with each other, forming Ca-O-Al cages and the framework of C12A7. C12A7 framework formation was initiated at 900°C -1000°C as detectable in the XRD pattern obtained at 900°C or above. Previous X-Ray diffraction measurements showed the increase in values of the crystallite size from 75nm to 145nm with the rise in annealing temperature from 900°C to 1200°C reducing the optical energy gap between the framework valence band and the cage conduction band [11]. The cubic crystal structure of C12A7 which is completely formed at 1100°C belongs to the $I\bar{4}3d$ space group.

The phase transitions and thermal associated reactions were found to be affected by the heating rate. The exothermic peaks due to CaO crystallisation and γ-Al_2O_3 to α-Al_2O_3 transformation were found to be shifting to higher temperatures as the heating rate was increased. This implies that the crystallisation is a thermally activated kinetic process [25]. The activation energy E_a for this

crystallisation process under nonisothermal conditions can often be described by the Kissinger equation in the form [26]:

$$\ln \frac{T_p^{\,2}}{\beta} = \ln \frac{E_a}{R\nu} + \frac{E_a}{RT_p} \qquad (1)$$

where β, T_p, R and ν are the heating rate, the peak temperature, the universal gas constant and the frequency factor, respectively.

The Kissinger plots of $\ln \frac{T_p^{\,2}}{\beta}$ against $\frac{1}{T_p}$ are shown in the inset of Figure 2. Values of E_a were estimated from the slope of the plots to be 348 kJ/mol and 375 kJ/mol for crystallisation of CaO and the γ-Al_2O_3 to α-Al_2O_3 transition, respectively. The value of $E_a = 348\,kJ/mol$ is consistent with the highly endothermic character of the overall decomposition of calcium nitrate [27]. The activation from γ-Al_2O_3 to α-Al_2O_3 represents the transformation from metastable to stable state and the value of E_a agrees well within the reported range [28]. The transition temperature, however, may be susceptible to various factors, such as purity, the degree of crystallinity and the presence of foreign ionic impurities [29,30].

3.2 FTIR and Raman Spectroscopy

FTIR measurements were carried out using two different samples; one with amorphous C12A7 dried gel and the other with crystallized C12A7 powder. Figure 3 shows the FTIR pattern for both samples, where the FTIR spectrum of amorphous C12A7 dried gel provides evidence of the presence of AlOOH, $Ca(NO_3)_2$, Etac and butoxy groups separated from Al atoms.

Table I shows the most characteristic bands for each of these compounds, followed by the corresponding Raman shifts. Hydrolysis of $Al(OBu)_2(Etac)$ is initiated by the separation of both Etac and butoxy groups attached to AlO. The observation of the absorption peaks at 1735 cm^{-1} and 1615 cm^{-1} corresponding to stretching vibrations of C-C bonds for free Etac groups in ketonic and enolic forms respectively, conclusively suggests that Etac is present in the dried gel as a separate phase in both possible forms [14]. If attached to AlO, Etac would be present only in enolic form. Comparing the FTIR spectra for amorphous and crystalline C12A7 provides evidence of the removal of all organic compounds as a result of thermal treatment. Such comparison is also an asset to demonstrate the cage formation in crystalline C12A7. Four

featured bands at 740, 815, 1060 and 1370 cm^{-1} in the FTIR pattern of amorphous C12A7 are assigned to Ca-O-NO_2 vibrations. As a bivalent metallic nitrate, $Ca(NO_3)_2$ follows a C_{2v} symmetry rather than the D_{3h} that would normally occur in monovalent metallic nitrates [31]. These absorption bands, as well as the ones in the range of 400-700 cm^{-1} arising from the presence of AlOOH, virtually disappear in the FTIR pattern of crystalline C12A7. Typical reported peaks for crystalline C12A7 phase are observed in our data. As stated above there is no evidence of individual Ca-O or Al-O bonding in the FTIR spectrum of crystalline C12A7. Ca, Al and O atoms are confined together to form the Ca-O-Al cage structure with the vibration peak at 530cm^{-1} exclusively. The peak at 790cm^{-1} is believed to be associated with the free oxygen ions (O_2^{2-}) which are trapped inside the cages [32]. Such phase transformation and crystallisation is also noticeable in the HTXRD pattern of amorphous to crystalline C12A7, providing more details about these phenomena. Finally the thermal treatment of C12A7 in air is favourable for incorporation of OH^- ions inside the cages. These ions are identified with the absorption band at 3620 cm^{-1}. The upshift of the absorption peaks due to OH vibration compared to hydroxyl groups in amorphous phase is believed to be due to the fact that OH^- ions inside the cage are loosely bound to cage wall, vibrating at lower energy levels and higher wavelengths [33].

All of the normal modes of vibration in a molecule cannot be excited by FTIR. Accordingly our FTIR experimental findings are supported and complemented by Raman spectroscopy that was carried out on the same samples as FTIR. Corresponding Raman shifts are presented in Table I, which are in complete agreement with FTIR data. Figure 4 and Figure 5 illustrate the Raman shifts due to the disappearance from the crystalline sample of organic and inorganic compounds that were present in amorphous dried gel. Two strong Raman shifts at 520nm and 780nm are visible in Figure 4 due to the crystal structure of C12A7. This pattern demonstrates that the thermal treatment was sufficient to remove all other compounds and form the desired bondings.

4 Conclusions

The sol-gel derived binary compound, C12A7 of the CaO-Al_2O_3 system was fabricated with precise control over the chemical composition of precursors, concentration of solvents and water and the pH of the sol. The high level of homogeneity and transparency of the C12A7 solution in ethanol was achieved by optimizing pH values, reaction dynamics and modified precursor structures. In-situ High Temperature X-Ray Diffraction (HTXRD) and Differential Scanning Calorimetry (DSC) studies on phase transformations of the C12A7 powder over wide range of

temperature from 25^0C to 1200^0C showed that the sample was amorphous at room temperature but it became completely crystallized on heat treatment at 1100°C for 3 hours. The exothermic peak temperatures due to crystallisation of γ-Al_2O_3 and its transformation to α-$Al2O_3$ were found to have risen with increase in the heating rate from 5°C/min to 20°C/min. The purity of the C12A7 and the removal of redundant chemical by-products were confirmed by independent Fourier Transform Infrared (FTIR) and Raman Spectroscopic measurements on amorphous and crystalline C12A7. In conclusion, heat treatment of sol-gel derived C12A7 shows 1100°C is the optimum temperature for complete crystallization.

Acknowledgements

The one of the authors (MZ) thank the LP Displays, Blackburn, UK for the PhD studentship with their financial support. This work was carried out at the School of Engineering and Materials Science of Queen Mary, University of London. We are also grateful to Dr Lesley Hanna of the Wolfson Centre for Materials Processing, Brunel University for fruitful discussions and input.

References

1 T. Kamiya, H. Hiramatsu, K. Nomura, H. Hosono, *J. Electroceram.* **17** (2006) 267.

2 J. E. Medvedeva, A. J. Freeman, *Europhysic. Lett*, **69 (**2005) 583.

3. K. Nomura, H. Ohta, K. Ueda, T. Kamiya, M. Hirano, H. Hosono, *Science* **300** (2003) 1269.

4. P. V. Shushko, A. L. Shluger, K. Hayashi, M. Hirano, H. Hosono, *Thin Solid Films*, **445 (**2003) 161.

5. P. V. Shushko, A. L. Shluger, K. Hayashi, M. Hirano, H. Hosono, *Phys. Rev. B,* **73** (2006) 014101.

6. P. M. Nikolic, D. Lukovic, S. Savic, D. Urosevic, S. Djuric, *Science of Sintering* **35** (2003)147.

7. H. Harimochi, J. Kitagawa, M. Ishizaka, Y. Kadoya, M. Yamanishi, S. Matsuishi, H. Hosono, *Phys. Rev. B,* **70** (2004) 193104.

8. M. Zahedi, A. K. Ray, D. S. Barratt, *Science of Advanced Materials* **1(2)** (2009) 107.

9. C.H. Jung, P.H. Tai,. Y.K. Kang, D.S. Jang, D.H. Yoon, *Surface and Coatings Technology*, **202** (2008) 5421.

10. A. C. Tas, *J.Am. Ceram. Soc*, **81** (1998) 2853.

11. M. Zahedi, A. K. Ray, D. S. Barratt, *J. Phys. D: Appl. Phys.,* **41** (2008) 035404

12. M. Zahedi, A. K. Ray, *J. Sol-Gel. Sci. Technol*, **55** (2010) 317.
13. N. B. Maharajan, N. S. Saxena, D. Bhandari, M. M. Imran, D. D. Paudya , *Bull. Mater. Sci.*, **23(5)** (2000) 369.
14. L. B. Coury, F. Babonneau , J. Livage, *J. sol-gel. Sci. Technol*, **3** (1994) 157.
15. J. Escobar, J. A. De Los Reyes, T. Viveros, *Applied Catalysis A: General*, **253** (2003) 151.
16. L. Shi, N. B. Wong, *J. Mater. Res*, **14** (1999) 3599.
17. X. Changrong, W. Feng, M. Zhaojing, L. Fanqing, P. Dingkun, M. Guangyao, *Journal of Membrane Science,* 116 (1**996**) 9.
18. J. Ma, C. H. Liang, L. B. Kong, C. Wang, *Journal of Materials Science: Materials in Medicine,* **14** (2003) 797.
19. A. Elliot, *Infrared Spectra and Structure of Organic Long-chain Polymers*, 1969, UK, Edward Arnold Ltd pp: 83-106.
20. E. Garreta, T. Fernandez, S. Borros, J. Esteve, C. Colominas, L. Kempf, *Mat. Res Soc. Symp. Proc.*, **724** (2002) 173.
21 A. K. Galwey, C. Ettarh, *Thermochimica Acta*, **316 (**1998) 57.
22. M. Thiruchitrambalam, V. R. Palkar, V. Gopinathan, *Mater. Lett*, **58 (**2004) 3063.
23. M. Mazloumi, R. Khalifehzadeh, S. K. Sadrnezhaad , H. Arami, *J. Am. Ceram. Soc*, **89** (2006) 3654.
24. K. Okada, A.Hattori, Y. Kameshima, A . Yasumori and R. N. Das, *J. Am. Ceram. Soc.*, 83 (2000) 1233.
25. Y. X. Zhuang, P. F. Xing, H. Y. Shi, J. Chen, P. W. Wang, J. C. He, *J. Appl. Phys.* **108** (2010) 033515 _
26. H.M. Kissinger, *Analytical Chem,* **29 (**1957**)**1702.
27, C, Ettarh and A.K . Galwey, *Thermochim. Acta,* 288 (1996) 203 **DOI:** 10.1016/S0040-6031(96)03052-3.
28. L. Baca, J. Plewa, L. Pach and J. Opfermann, *J. Therm. Anal. Calorim.* 66 (2001) 803 **DOI:** 10.1023/A:1013148223203
29. K. Okada, A. Hattori, Y. Kameshima and A. Yasumori, *Mater. Lett.* 42 (2000) 175.
30. F. Nahif, , D. Music, S. Mraz, M. T. Baben and J. M. Schneider, *J. Phys.-Condes. Matter* 25 (2013) **Article Number:** 125502 **DOI:** 10.1088/0953-8984/25/12/125502
31. S. D. Ross, *Inorganic Infrared and Raman Spectroscopy*,1972, UK, McGraw-Hill Book

Company Ltd, pp: 95-112.

32. D. Wang, Y. X. Liu, C.S. Xu, Y. C. Liu, G. R. Wang, X. H. Li, *J. Rare Earths*, **26** (2008) 433.

33. K. Nakanishi, *Infrared Absorption Spectroscopy*,1962, Japan, Nankodo Company Ltd .

Table Caption:

Table I – Featured FTIR Absorption bands (cm^{-1}) of FTIR pattern illustrated in figure 3 and Raman shifts (cm^{-1}) for Raman spectroscopy with different laser intensities at 532nm and 785nm illustrated in figures 4 and 5, showing the main peaks for each compounds present in amorphous and crystalline C12A7.

Figure Captions:

Figure 1: HTXRD pattern of C12A7. The data were collected in the sequence every 100°C of thermal treatment from room temperature to 1200°C. The insets on the right show the featured diffractions due to calcium nitrate at 400°C and C12A7 at 1100°C. The diffraction pattern provides no evidence of crystallisation of AlOOH.

Figure 2: DSC pattern of C12A7 dried gel heated at the rate of (a) 5°C/min (b) 10°C/min and (c) 20°C/min from room temperature to 1200°C. Inset showing Kissinger plots for CaO crystallisation (■) and (●) γ-Al_2O_3 to α-Al_2O_3 transformation.

Figure3: FTIR spectra of (a) amorphous C12A7 dried gel and (b) crystalline C12A7 powder exposed to thermal treatment at 1100°C for 3 hours. Spectrum (a) contains all the bands due to AlOOH, $Ca(NO_3)_2$, Etac and butoxy groups. The disappearance of all these bands in spectrum (b) demonstrates how the Ca-Al-O cages are formed with O^{2-} ions trapped inside.

Figure 4: Raman pattern of two phases of C12A7, Trace (a) shows the amorphous C12A7 dried gel and trace (b) shows the same dried gel after thermal treatment at 1100°C for 3 hours. Spectrum (a) contains featured bands due to organic and inorganic compounds in C12A7 dried gel while spectrum (b) confirms the removal of all the mentioned compounds followed by the vibrations due to Ca-Al-O framework and O^{2-} ions trapped inside. (The spectra were obtained using a laser beam with the intensity of 532nm).

Figure 5: Raman pattern of two phases of C12A7, Trace (a) shows the amorphous C12A7 dried gel and trace (b) shows the same dried gel after thermal treatment at 1100°C for 3 hours. (The spectra were obtained using a laser beam with the intensity of 785nm).

Table I

Compound	FTIR	Raman (532nm)	Raman (785nm)	Bonding	References
$Ca(NO_3)_2$	740	740	740	Ca-O-No_2(C_{2v} symmetry)	[16], [17]
	815	-	815	Ca-O-No_2(C_{2v} symmetry)	[16], [17]
	1060	1050	1050	Ca-O-No_2(C_{2v} symmetry)	[16], [17]
	1370	1360	1360	Ca-O-No_2(C_{2v} symmetry)	[16], [17]
Boehmite (AlOOH)	420	425	425	Al-O vibration	[18], [19]
	520	-	520	Al-O vibration	[18], [19]
	620	610	610	Al-O vibration	[18], [19]
	740	740	740	Al-O vibration	[18], [19]
	980	980	980	Bending vibration of OH	[18], [19]
	1020	-	-	Bending vibration of OH	[18], [20]
	1060	1050	1050	Bending vibration of OH	[18], [20]
	3500	3500	-	Stretching vibration of OH	[18], [20]
Ethyl acetoacetate	1170	1170	1170	Stretching vibration of C-H	[10], [17]
	1300	1300	1300	Bending vibration of C-C	[10], [17]
	1370	1360	1360	Stretching vibration of CH_3	[10], [17]
	1420	1420	1420	Stretching vibration of CH_3	[10], [17]
	1520	1520	1520	Bending vibration of C=C	[10], [17]
	1615	1620	-	Stretching vibration of C-O for enolic form	[10]
	1735	-	-	Stretching vibration of C-O for ketonic form	[10]

	2920	2920	2920	vibration of CH_2	[10], [17]
	2980	2980	-	vibration of CH_2	[10], [17]
Butoxy ligands	1060	1050	1050	Stretching vibration of C-O	[17]
	1370	1360	1360	Stretching vibration of CH_3	[17]
	1420	1420	1420	Stretching vibration of CH_3	[17]
	2920	2920	2920	vibration of CH_2	[17]
	2980	2980	-	vibration of CH_2	[17]
C12A7	530	520	520	Vibration of C12A7 lattice framework	[18]
	790	780	780	Vibration of O^{2-} ions	[18]
	3620	3620	-	Bending vibration of OH^-	[17], [20]
	3650	3660	-	Bending vibration of OH^-	[17], [20]

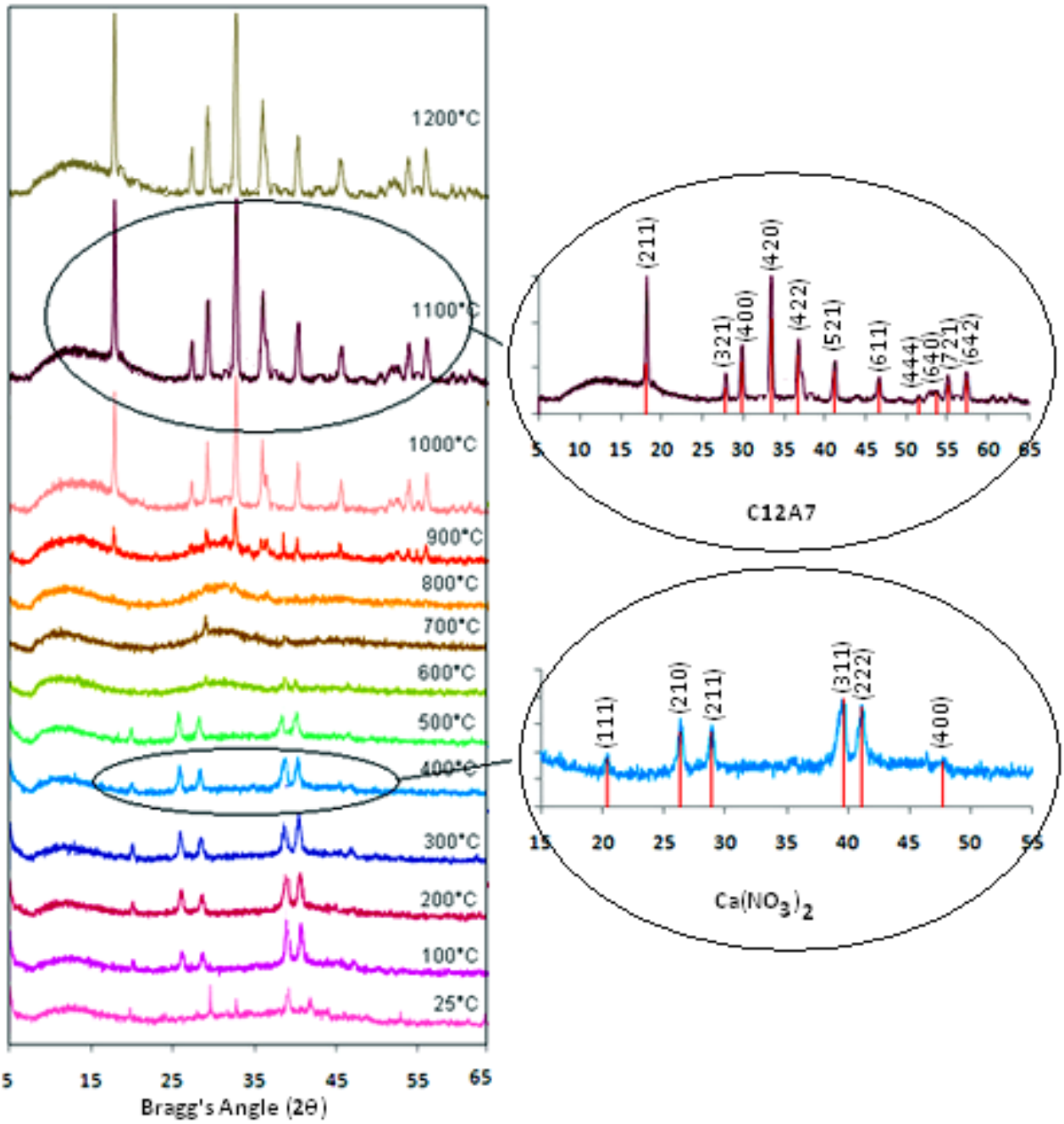

Figure 1 – HTXRD pattern of C12A7. The data were collected in the sequence every 100°C of thermal treatment from room temperature to 1200°C. The insets on the right show the featured diffractions due to calcium nitrate at 400°C and C12A7 at 1100°C. The diffraction pattern provides no evidence of crystallisation of AlOOH.

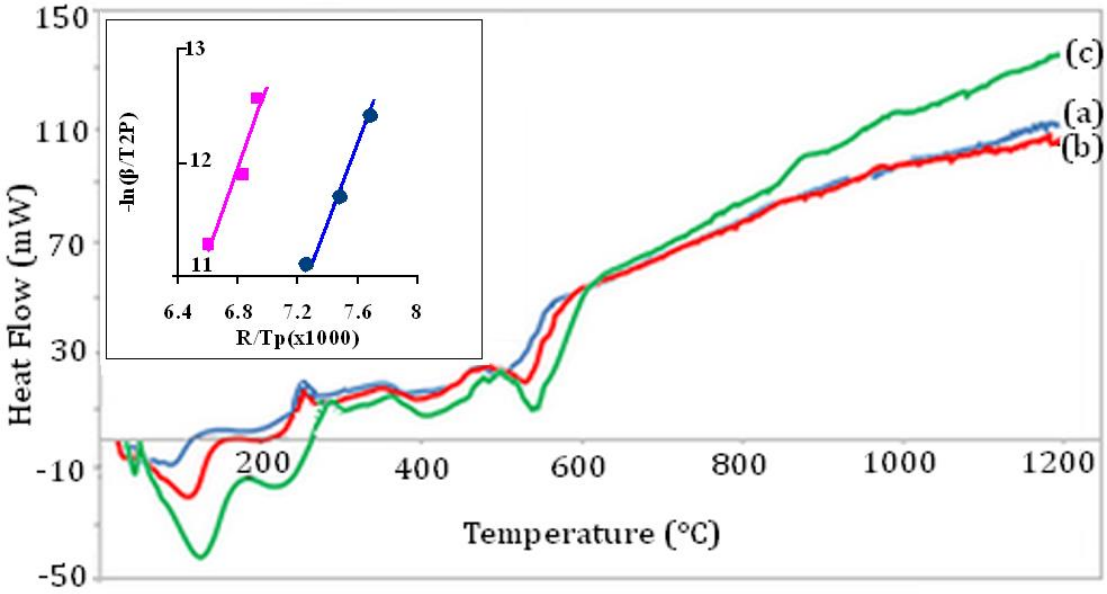

Figure 2 - DSC pattern of C12A7 dried gel heated at the rate of (a) 5°C/min (b) 10°C/min and (c) 20°C/min from room temperature to 1200°C. Inset showing Kissinger plots for CaO crystallisation (■) and (•) γ-Al_2O_3 to α-Al_2O_3 transformation.

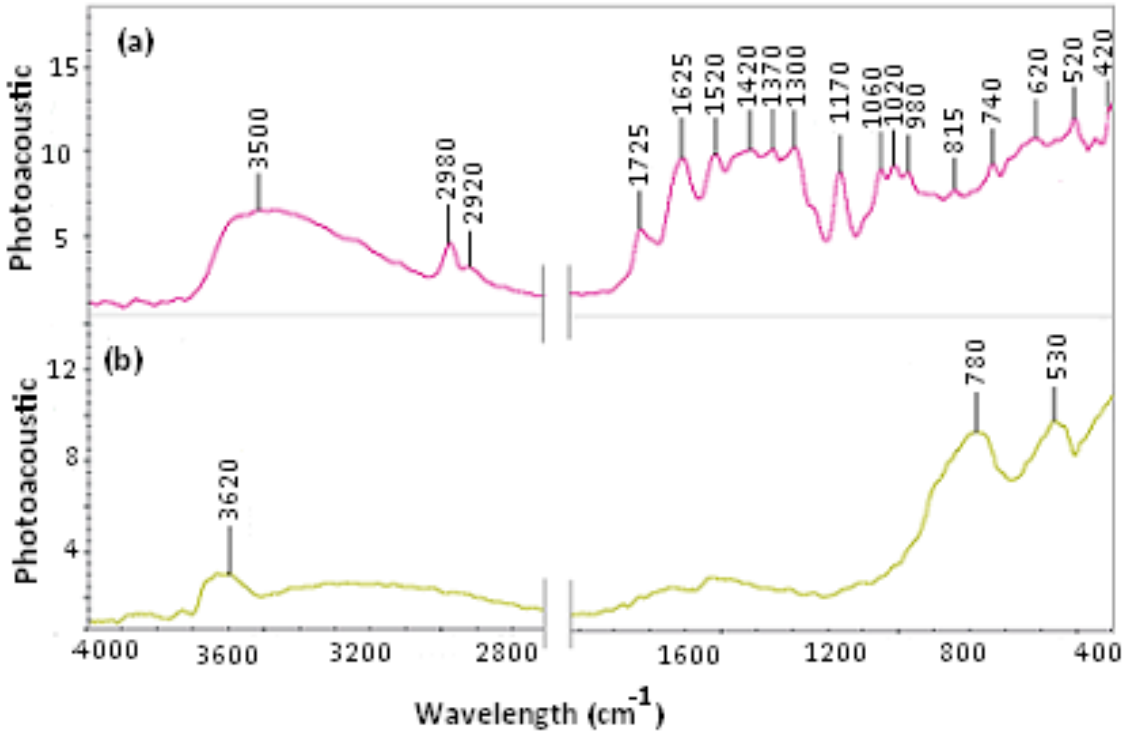

Figure3- FTIR spectra of (a) amorphous C12A7 dried gel and (b) crystalline C12A7 powder exposed to thermal treatment at 1100°C for 3 hours. Spectrum (a) contains all the bands due to AlOOH, $Ca(NO_3)_2$, Etac and butoxy groups. The disappearance of all these bands in spectrum (b) demonstrates how the Ca-Al-O cages are formed with O^{2-} ions trapped inside.

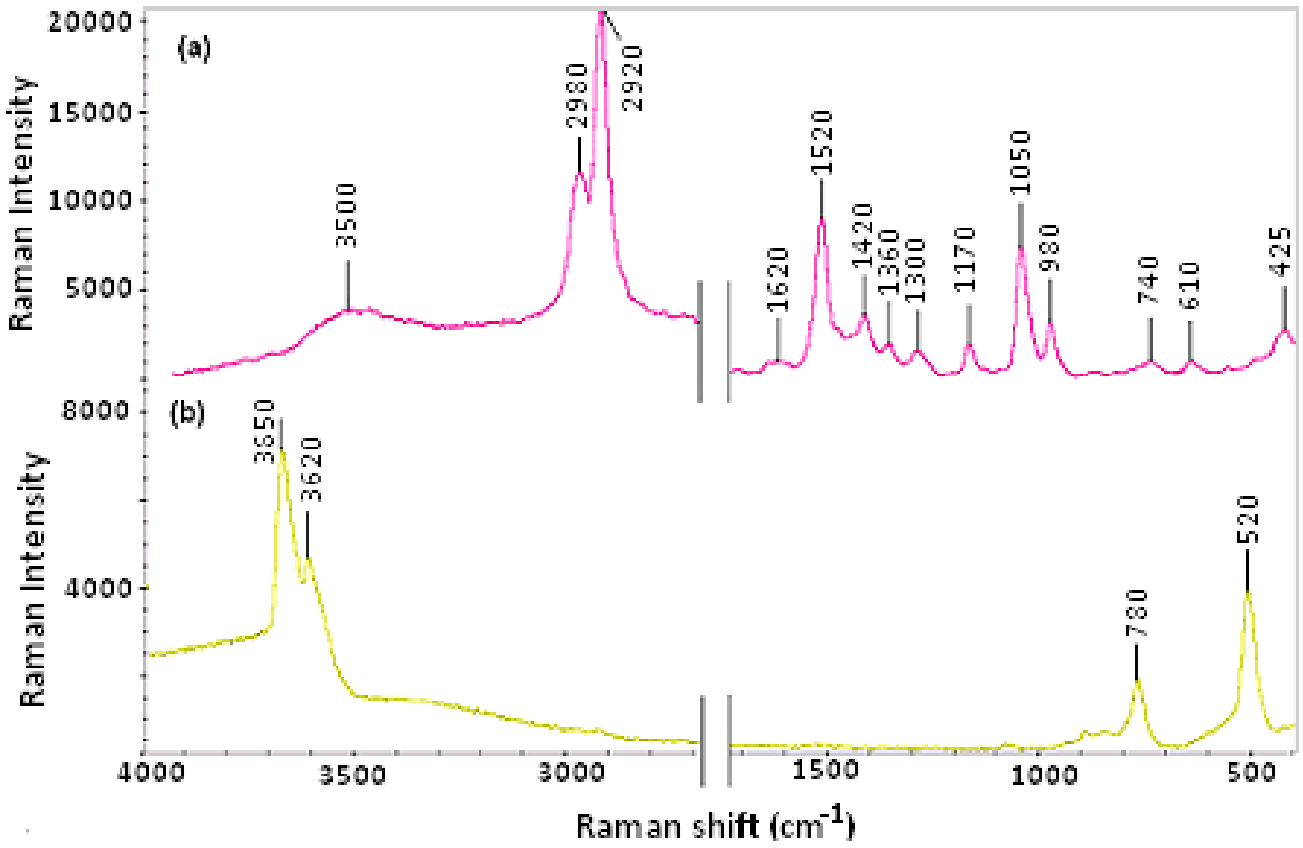

Figure 4- Raman pattern of two phases of C12A7, Trace (a) shows the amorphous C12A7 dried gel and trace (b) shows the same dried gel after thermal treatment at 1100°C for 3 hours. Spectrum (a) contains featured bands due to organic and inorganic compounds in C12A7 dried gel while spectrum (b) confirms the removal of all the mentioned compounds followed by the vibrations due to Ca-Al-O framework and O^{2-} ions trapped inside. (The spectra were obtained using a laser beam with the intensity of 532nm).

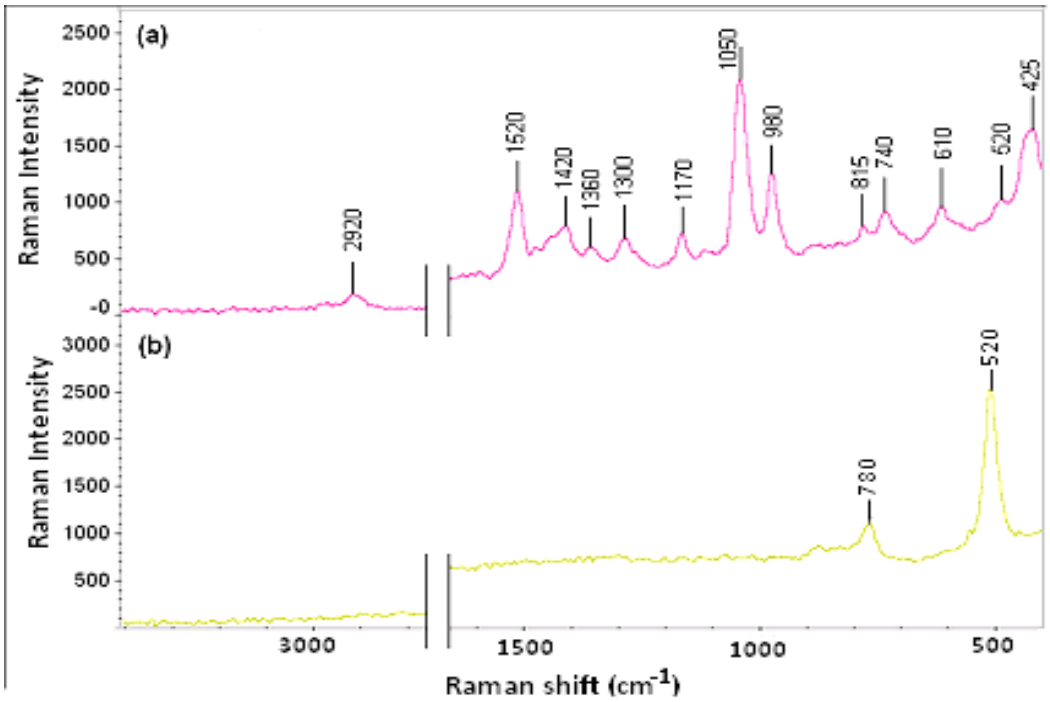

Figure 5- Raman pattern of two phases of C12A7, Trace (a) shows the amorphous C12A7 dried gel and trace (b) shows the same dried gel after thermal treatment at 1100°C for 3 hours. (The spectra were obtained using a laser beam with the intensity of 785nm).